MALAYSIAN JOURNAL OF MICROSCOPY

Journal homepage: https://malaysianjournalofmicroscopy.org

RESEARCH ARTICLE

COMPARISON ON STRUCTURAL, MORPHOLOGICAL AND ELECTRICAL ANALYSIS ON Mn AND Zn-DOPED KNN THIN FILM BY SOL-GEL METHOD

Muhd Afiq Hafizuddin Azman[1], Hidayah Mohd Ali Piah[1], Mohd Warikh Abd Rashid[1,*], Umar Al-Amani Haji Azlan[1], Maziati Akmal Mat Harttar@Mohd Hatta[2], Toshihiro Moriga[3]

[1]Faculty of Industrial and Manufacturing Technology and Engineering, Universiti Teknikal Malaysia Melaka, Hang Tuah Jaya, 76100 Durian Tunggal, Melaka, Malaysia.

[2]Faculty of Engineering, International Islamic University Malaysia, 53100 Jalan Gombak, Kuala Lumpur, Malaysia

[3]Department of Chemical Science and Technology, Graduate School of Advanced Technology and Science, Tokushima University, 2-1 Minami-Josanjima, Tokushima, 770-8506 Japan.

Abstract. The lead-free sodium potassium niobate (KNN) exhibits improved electrical and structural properties. This substance is well-known because it resembles lead zirconate titanate (PZT). KNN may replace the commonly used PZT, although it has significant drawbacks. This study introduced metal oxide doping. The perovskite structure of KNN contained manganese oxide (MnO) and zinc oxide (ZnO) dopants. The improved electrical characteristics of KNN thin films doped with MnO and ZnO were investigated by studying the effects of manganese and zinc dopants on the surface morphology and resistivity. The chemical solution deposition was used as methodology. Their structural, morphology and electrical properties of the doped KNN thin film were analysed using X-ray Diffraction (XRD), Field Emission Scanning Electron Microscopy (FESEM), and LCR meter. The peak of all KNN thin films was in the (001), indicating a preferred for growth orientation. Mn-doped KNN films had improved crystallinity and suppressed secondary phases, while ZnO doping preserved the crystal structure with only minor disturbances. The microstructure of Mn-doped KNN thin films was homogeneous and dense with reduced grain boundaries, while Zn-doped KNN thin films had a denser morphology and bigger grain sizes, especially at higher doping levels. The electrical measurements showed that Mn doping increases resistivity, making films better for high-performance piezoelectric applications. Conversely, the incorporation of zinc resulted in a reduction in the electrical resistance of the material as its concentration increased. The work shows that Mn and Zn doping affects KNN thin film structural, morphological, and electrical properties differently. The results showed that MnO-doped KNN performed best at a concentration of 0.3 mol and ZnO-KNN at 0.9 mol. These results aid the development of improved KNN-based materials for electrical and piezoelectric applications.

Keywords: KNN, thin film, doped, structural.

Article Info

Received 22 February 2025
Accepted 14 May 2025
Published 2 June 2025

***Corresponding author: warikh@utem.edu.my**

ISSN: 1823-7010, eISSN: 2600-7444

1. INTRODUCTION

Potassium sodium niobate (KNN), (K_xNa_{1-x}) NbO_3 thin films have garnered significant attention in the field of materials science due to their excellent piezoelectric and ferroelectric properties, which make them suitable for a wide range of applications, including sensors, actuators, and energy harvesting devices. It features an ABO_3 perovskite crystal structure, where potassium (K^+) and sodium (Na^+) occupy the A-site, while niobium (Nb^{5+}) sits at the B-site, surrounded by an oxygen octahedral coordination. However, the addition of dopants like Mn, Zn, or Li can further improve its piezoelectric and electrical properties by enhancing grain growth, reducing leakage current, and optimizing domain configurations. Among these, manganese (Mn) and zinc (Zn) have emerged as promising dopants due to their potential to improve the structural and electrical properties of KNN thin films [1-3]. Researchers rely on several scientific factors, including ionic compatibility, defect engineering, phase stabilization, and electrical conductivity improvements, to justify their choice.

Previous research has shown that doping KNN thin films with transition metals can significantly alter their properties. For instance, Mn doping has been shown to improve the ferroelectric and piezoelectric properties of KNN thin films by enhancing their crystallinity and reducing leakage current [4]. On the other hand, Zn doping is known to influence the grain size and surface morphology, which can affect the films' dielectric properties [5]. However, the study is a comparison of the effect of impurities on the properties of KNN.

Among various synthesis techniques, the sol-gel method has proven to be a particularly effective approach for fabricating high-quality KNN thin films. This wet chemical process enables precise control over stoichiometry, uniform mixing of precursors at the molecular level, and deposition over large areas at relatively low temperatures. Several studies have demonstrated the viability of sol-gel-derived KNN films in achieving uniform microstructures and desirable functional properties. For example, Zhang et al. [6] successfully synthesized crack-free KNN thin films using the sol-gel spin-coating method and demonstrated good ferroelectric behaviour with well-saturated polarization loops. Their study highlighted the importance of optimizing annealing temperatures and film thickness to enhance phase purity and electrical response. In another significant work, Wiegand et al. [7] explored the impact of different heat-treatment profiles on the crystallization behaviour of sol-gel derived KNN thin films. They found that slow ramping and controlled calcination steps contributed to improved grain growth and texture development, which are essential for optimal piezoelectric activity. Moreover, the study underlined how processing conditions such as drying atmosphere and precursor aging time could influence the final film quality.

Doping studies using the sol-gel technique have also become increasingly common in recent years. For instance, Lai et al. [8] investigated lithium-doped KNN thin films prepared by the sol-gel route, reporting that Li incorporation not only enhanced densification and reduced porosity but also promoted the formation of a stable orthorhombic phase favourable for high piezoelectric response. Similarly, Sun et al. [9] examined the effect of Mn doping on sol-gel-derived KNN films and observed a notable improvement in leakage current suppression and ferroelectric loop squareness, attributing these results to defect compensation and improved crystallite alignment.

Overall, this study systematically compares Mn- and Zn-doped KNN thin films synthesized via the sol-gel method, focusing on their structural, morphological, and electrical properties. By preparing KNN thin films with varying concentrations of Mn and Zn dopants, the research aims to elucidate the comparative effects of these dopants on film performance. Characterization techniques such as X-ray diffraction (XRD), field emission scanning electron microscopy (FESEM), and electrical measurements will be employed to analyse phase composition, microstructure, and conductivity. The primary objective is to understand the mechanisms by which Mn and Zn influence KNN thin films and to determine optimal doping conditions for enhanced functional properties. Ultimately, this study contributes to the development of high-performance KNN-based devices for applications in piezoelectric sensors, actuators, and energy harvesting technologies by providing insights into dopant-induced modifications in KNN thin films.

2. MATERIALS AND METHODS

Figure 1 illustrates the flowchart of the fabrication process of manganese and zinc-doped KNN (potassium sodium niobate) thin films at doping concentrations of 0.3 mol and 0.9 mol, respectively, on a silicon substrate using the sol-gel method. The sol-gel chemical solution deposition (CSD) method as shown in Figure 2 is commonly used to fabricate KNN thin films. Potassium acetate (CH_3COOK) and sodium acetate (CH_3COONa) are utilized as alkaline precursors in the initial solutions. To address the deficiency of alkaline elements, varying amounts of manganese and zinc (0.3 mol and 0.9 mol) were incorporated into the precursor solutions. These compounds were dissolved in the polar organic solvent 2-MOE, with continuous stirring at room temperature. Subsequently, niobium ethoxide, 2-MOE, and acetylacetone were combined to create a niobium precursor solution. Acetylacetone functions as a chelating agent, improving the solution's stability against hydrolysis. The previously prepared KNN precursors were then mixed with the niobium solution. The mixed solution was maintained at 80 °C for one hour.

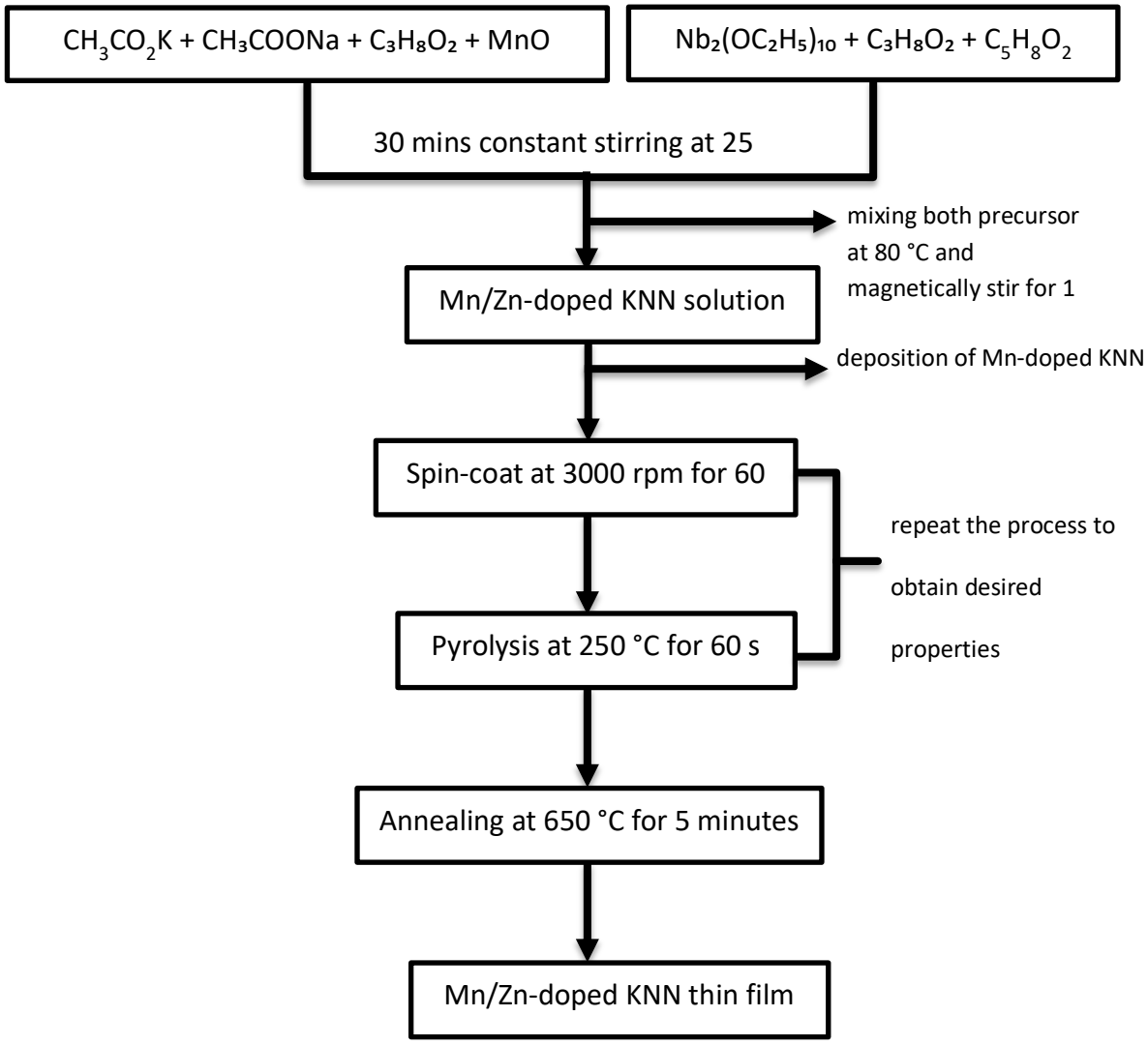

Figure 1: Flowchart of fabrication on Manganese/Zinc-doped Potassium Sodium Niobate (KNN) thin film via sol-gel method

Silicon substrate was cut into a dimension of 1 cm by 1 cm, which was then submerged in acetone and subjected to ultrasonic agitation for 20 minutes. The substrates were subsequently cleaned

and rinsed with deionized water after a 20-minute immersion in ethanol. Finally, the substrates were purged with nitrogen gas to remove any residual impurities.

The Mn/Zn-doped KNN solution was applied to the Si substrate using a spin coater, spinning at 3000 rpm for 60 seconds. The substrate was then subjected to heat treatment at 250 °C for one minute on a hot plate immediately after spin coating. The selected pyrolysis temperature is attributed to achieving a higher degree of crystallinity because it facilitates the removal of organic residues, promotes nucleation, and enhances grain growth. The spin coating process was conducted five more times to achieve the desired multi-layered thin film, thereby improving homogeneity and uniformity. The furnace temperature was then adjusted to 650 °C for 5 minutes to initiate the annealing process.

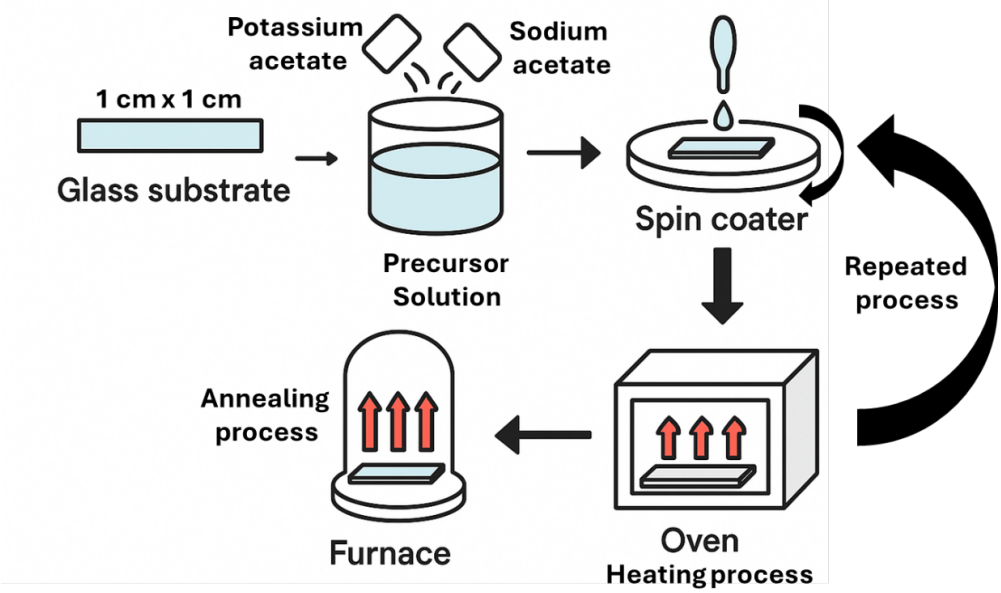

Figure 2: Sol-gel process method

XRD was used to analysis the crystal structure of the KNN thin films that has been doped with manganese and zinc. CuKα radiation with a wavelength of 1.54 Å was utilized to measure the diffraction angle within the range of 20° to 60° (2θ). FESEM was used to analyse the surface structure and determine the chemical composition of the deposited thin films. The samples were coated with a thin layer of gold to enhance conductivity. FESEM images were taken at magnifications ranging from 50,000x. The resistivity of the thin film was analysed using a LCR meter (U1733C Agilent Technologies) operating at room temperature with a testing frequency of 1 kHz. Four-point resistivity probe measurement (I-V Keithly) was used to measure the resistivity of KNN thin films. The measurement of current will pass through the two outer probes and the voltage will measure by inner probes that allow the measurement of the thin film's resistivity.

3. RESULTS AND DISCUSSION

3.1 X-ray Diffraction (XRD)

In term of phase composition, the XRD pattern of the 0.3 mol Mn-doped KNN thin film typically shows peaks corresponding to the perovskite structure of KNN, $(K_xNa_{1-x})\ NbO_3$. The presence of Mn at 0.3 mol doping does not significantly alter the main phase but can introduce slight peak shifts or broadening due to the lattice distortion or the incorporation of Mn ions into the KNN lattice as shown in Figure 3. Mn doping at this level might result in slight changes in the lattice parameters compared to undoped KNN in term of lattice parameters. The ionic radius of Mn is slightly smaller than that of the ions it replaces (K^+, Na^+, or Nb^{5+}), leading to a minor contraction of the lattice [10]. The preferred

orientation (texture) of the thin film might show a similar trend to undoped KNN, but slight changes could occur due to the Mn doping.

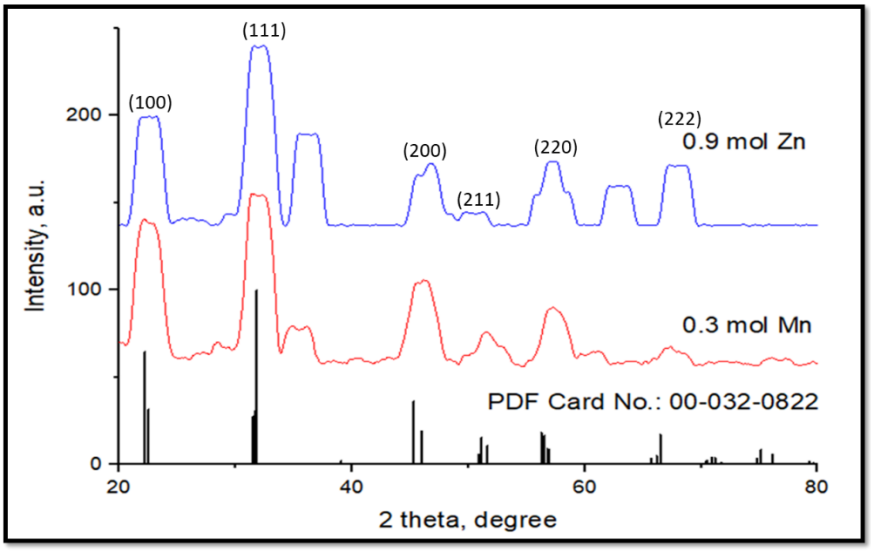

Figure 3: XRD patterns of 0.3 mol Mn and 0.9 mol Zn-doped KNN thin films

In addition, the XRD pattern of the 0.9 mol Zn-doped KNN thin film also exhibits peaks corresponding to the perovskite structure of KNN. At 0.9 mol doping, Zn incorporation can lead to more noticeable changes in the diffraction pattern compared to lower doping levels. The emergence of supplementary peaks at specific 2θ positions, particularly at of 47°, 52° and 56°, in the samples infused with 0.9 mol ZnO, further substantiates the existence of a ZnO phase. The existence of these peaks serves as evidence for the development of a pure orthorhombic perovskite structure, devoid of any secondary phase [11-13]. In term of lattice parameters, Zn doping at 0.9 mol is likely to cause more significant changes in the lattice parameters compared to 0.3 mol Mn doping. Moreover, this discovery indicates that the KNN lattice sites were effectively doped with zinc oxide, but the native phase remained intact.

The ionic radius of Zn^{2+} is different from those of K^{+}, Na^{+}, and Nb^{5+}, leading to either lattice expansion or contraction depending on the site of substitution. The crystallinity of the 0.9 mol Zn-doped KNN thin film might be slightly lower compared to the Mn-doped film due to higher doping levels, which Mn can enhance the crystallinity of doped KNN thin films [14]. Besides, peak broadening could be more pronounced, indicating low intensity of crystallinity. The preferred orientation might show more significant deviations from the undoped KNN thin film due to the higher doping concentration of Zn. Furthermore, changes in texture can affect the material's properties, and these would be more evident at higher doping levels.

3.2 Energy-dispersive X-ray Analysis (EDX)

The films' chemical composition was confirmed using Energy Dispersive X-ray Spectroscopy (EDX). Figure 4 presents the EDX analyses of Mn and Zn-doped KNN thin films deposited on ITO substrates and annealed at 650 °C. EDX results indicated the presence of Mn, K, Na, and Nb elements in the Mn-doped KNN thin film, as well as Si from the substrates.

These ions readily volatilized during the heating process. The incorporation of manganese as a dopant in the thermal process can mitigate the volatilization of potassium and sodium. The influence of solution conditions on the properties of sol-gel technique derived by KNN thin films on platinized sapphire substrates has been previously documented [15-16].

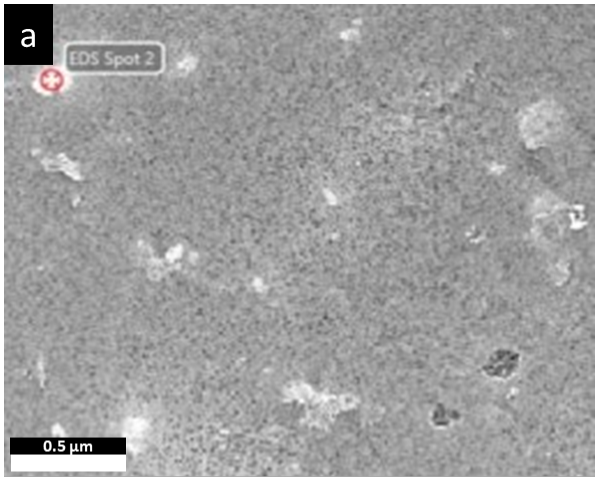

Element	Weight%	Atomic%
Na	15.7	28.2
O	38.35	31.45
Mg	1.2	2.1
Al	0.7	1.0
Si	11.0	16.15
K	1.6	1.7
Ca	4.0	4.2
Mn	10.25	7.7
Nb	17.1	7.6

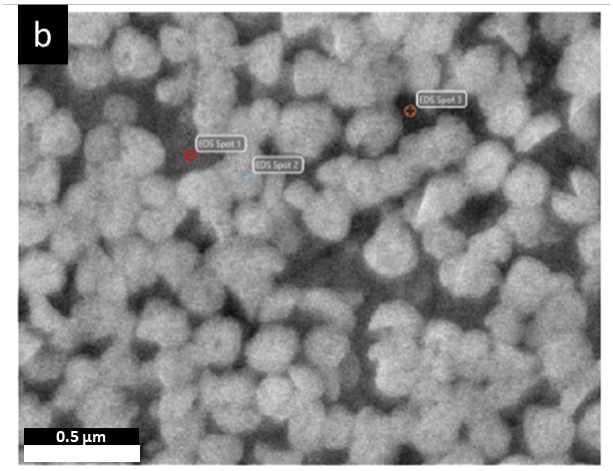

Element	Weight%	Atomic%
C	15.0	26.5
O	40.8	53.8
Na	5.3	4.9
Si	7.0	5.3
K	0.4	0.2
Ca	1.5	0.8
Zn	18.1	5.8
Nb	11.8	2.7

Figure 4: EDX analysis of KNN thin film deposited on Si substrate after sintering at 650 °C (a) 0.5 mol Mn, and (b) 0.9 mol ZnO

The chemical homogeneity of Mn-doped KNN thin films, with respect to Mn, Nb, and alkali elements, was assessed using EDX analysis. This technique quantified the amounts of Mn, Na, K, and Nb in Mn-doped KNN thin films at various concentrations. As shown in the table in Figure 4(a), Nb exhibited the highest atomic and weight percentages, followed by Na, Si, Mn, K, and Al, in that order regardless of the absence of O. Given the uniformity of Nb concentration across all films, it can be inferred that the influence of microstructural characteristics on the EDX mapping is minimal [17]. Films exhibiting alkali chemical inhomogeneity demonstrated greater fluctuations in grain size. Uniform grain size appears to be indicative of the chemical homogeneity of the films. Additionally, as shown in Figure 4(b), the elements C, O, Na, Si, K, Ca, Zn, and Nb were detected. The pure KNN thin film displayed the presence of its constituent elements potassium (K), niobium (Nb), sodium (Na), and oxygen (O). The analysis successfully identified the formation of an additional zinc (Zn) line following the introduction of the zinc element. However, the primary signal from the substrate, particularly in the case of silicon, was more prominent than the excited spectra of the essential components. This prominence is attributed to the film's thickness being less than the penetration depth of the incident electrons, resulting in the Si substrate being evident on the thin film's surface.

3.3 Field Emission Scanning Emission Microscopy (FESEM) Analysis

Figure 5 shows the comparison on the morphology of 0.3 mol Mn-doped and 0.9 mol Zn-doped KNN thin films using Field Emission Scanning Electron Microscopy (FESEM). Both doping elements, Mn and Zn, were chosen to investigate their effects on the microstructure and surface morphology of KNN thin films, which are known for their piezoelectric properties. For the sample preparation, KNN

thin films were prepared via so-gel spin coating technique. Doping concentrations were set to 0.3% for Mn and 0.9 mol for Zn. The films were annealed at 650 °C for 1 hour to crystallize the perovskite structure. Surface morphology, grain size and porosity were the primary focus on the FESEM analysis.

Figure 5(a) illustrated the surface morphology of the 0.3 mol Mn-doped KNN film displayed a relatively uniform surface with well-defined grains boundaries. Grains were mostly spherical and densely packed. Some porosity was observed but was minimal. Few pores were visible, suggesting good densification and the overall porosity was less than 5%. FESEM image of the 0.9 mol ZnO-doped KNN film, illustrated in Figure 5(b), demonstrates notable alterations in morphology. At 0.9 mol of ZnO doping, the microstructure exhibited improved compaction. This observation suggests that the films consisted solely of a single perovskite phase. Previous studies have demonstrated that the introduction of dopants into ZnO results in improved films characterized by a refined structure and heightened density. This enhancement is believed to result from a decrease in the volatility of alkaline compounds [18].

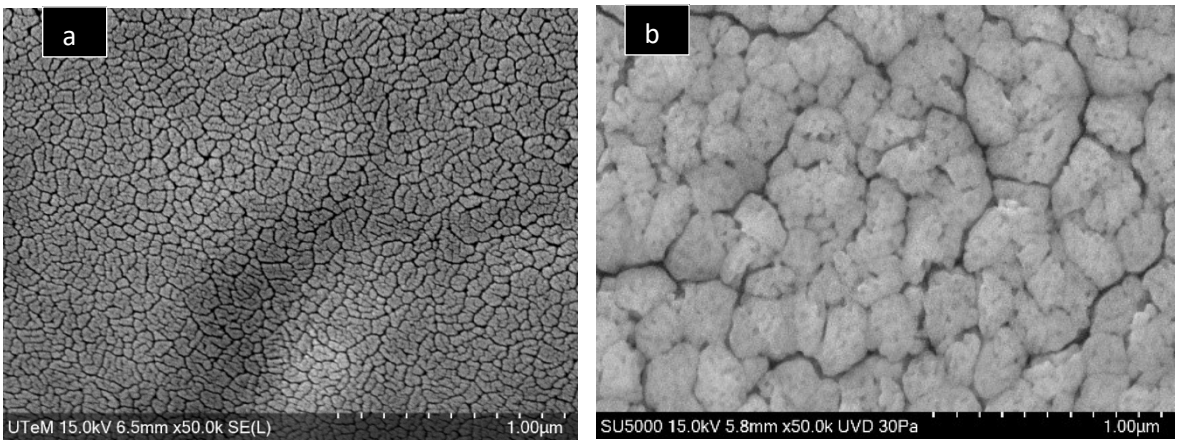

Figure 5: FESEM microstructure 0.3% of doped (a) manganese and 0.9% of doped, and (b) zinc KNN thin film via sol-gel method at x50.0k magnification

Mn-doping at 0.3% resulted in a more uniform and denser microstructure, suggesting Mn ions act as a grain growth inhibitor, leading to smaller grain sizes and lower porosity [19]. Zn-doping at 0.9 mol led to larger, irregular grains and denser morphology. In addition, Zn ions possibly promote grain growth and enhance densification, resulting in a rougher surface morphology. The observed differences in morphology are likely to influence the piezoelectric properties of the films.

FESEM analysis reveals significant differences in the surface morphology of 0.3 mol Mn-doped and 0.9 mol Zn-doped KNN thin films. Mn-doping tends to produce a more uniform and densely packed microstructure, while Zn-doping results in a rougher surface with dense and compact microstructure. These morphological differences are crucial for optimizing the functional properties of KNN thin films for specific applications. Further investigations into the electrical and piezoelectric properties of these doped films are recommended to correlate the morphological findings with performance metrics.

3.4 Resistivity

Table 1 shows that a 0.9% Zn-doped KNN thin film exhibits a higher resistivity compared to the 0.3% Mn-doped KNN thin film when measured at room temperature with a frequency of 1 kHz. Table 1 provides a comparative analysis of the resistivity of materials doped with manganese and zinc at different concentrations. Manganese, with a doping concentration of 0.3 mol, exhibits a resistivity of 0.03 MΩ. On the other hand, zinc, at a higher concentration of 0.9 mol, shows a significantly lower resistivity of $3x10^{-7}$ MΩ. This stark contrast in resistivity values indicates that zinc is a far more effective dopant for reducing resistivity compared to manganese. The higher concentration of zinc correlates with a dramatic decrease in resistivity, suggesting that zinc atoms integrate more efficiently

into the material's lattice, thereby enhancing its electrical conductivity [20]. Conversely, the relatively higher resistivity observed with manganese doping could be due to less effective integration or different interaction mechanisms within the material. Overall, the data underscores the importance of both the type and concentration of dopants in tailoring the electrical properties of materials, with zinc proving to be a superior choice for applications requiring low resistivity.

Table 1: Resistivity of Mn and Zn-doped KNN thin film at 0.3 mol and 0.9 mol respectively, at 1 kHz

Type of Dopant	Content, mol	Resistivity, MΩ
Manganese	0.3	0.03
Zinc	0.9	$3x10^{-7}$

Meanwhile, the FESEM analysis showed that increasing ZnO concentration at 0.9 mol as a dopant produced grains with better density and homogeneity. At concentrations 0.9 mol ZnO, the microstructure showed improved compaction and a thick film border. FESEM images of morphological surfaces show increased crystallite size and wide grain boundaries, indicating this occurrence. As ZnO doping increases, resistivity drops considerably, making the material more conductive [21]. ZnO can form a continuous phase or radically modify KNN's electronic structure at high concentrations, leading the material to behave like a ZnO-dominant compound, which has lower resistance. Adding 0.6 mol of ZnO reduced resistivity because substituted Zn ions at A-sites produce multiple electrons. It is claimed that minimising oxygen vacancies reduces resistivity by lowering electron scattering. As film grain size grows, electron concentration rises, lowering resistivity [22].

4. CONCLUSIONS

In conclusion, the comparative analysis of 0.3 mol Mn-doped KNN and 0.9 mol Zn-doped KNN thin films fabricated via the sol-gel method reveals distinct differences in their structural and electrical properties. X-ray diffraction (XRD) patterns indicate that both doped KNN thin films exhibit a perovskite crystal structure, but with notable variations in peak intensities and positions, suggesting different levels of crystallinity and lattice distortions due to the differing dopant concentrations and types. FESEM images showed Mn-doped KNN thin films have a relatively uniform and dense morphology, whereas Zn-doped KNN films display a more granular surface with larger grain sizes, indicating that Zn dopant influences the grain growth and surface roughness more significantly. Electrical analysis using an LCR meter reveals that the Mn-doped KNN thin films exhibits higher dielectric constants and better ferroelectric properties compared to the Zn-doped counterparts, which could be attributed to the more uniform microstructure and higher crystallinity. The distinct differences in structural, morphological, and electrical properties between Mn and Zn-doped KNN thin films highlight the impact of dopant type and concentration on the material's performance, providing valuable insights for tailoring the properties of KNN-based thin films for specific applications in electronic and ferroelectric devices.

Acknowledgements

The authors extend their appreciation to the Ministry of Higher Education, Malaysia, for funding this research work, grant no: FRGS/1/2021/TK1/UTEM/01/2.

Author Contributions

All authors contributed toward data analysis, drafting, and critically revising the paper and agree to be accountable for all aspects of the work.

Disclosure of Conflict of Interest

The authors have no disclosures to declare.

Compliance with Ethical Standards

The work is compliant with ethical standards.

References

[1] Afiq, H. A. M., Warikh, A. R. M., Azlan, U. A. A., Akmal, M. M. & Moriga, T. (2024). Synthesis and characterization of Mn-doped Potassium Sodium Niobate (KNN) thin film. *Journal of Advanced Manufacturing Technology (JAMT)*, 18(2), 1-16.

[2] Güneri, E., Henry, J., Göde, F. & Özpozan, N. K. (2023). Structural and optical properties of chemically deposited Mn-doped ZnO thin films. *Journal of Central South University*, 30(3), 691-706.

[3] Gültekin, Z., Alper, M., Hacıismailoğlu, M. C. & Akay, C. (2023). Effect of Mn doping on structural, optical and magnetic properties of ZnO films fabricated by sol–gel spin coating method. *Journal of Materials Science: Materials in Electronics*, 34(5), 438.

[4] Kovacova, V., Yang, J. I., Jacques, L., Ko, S. W., Zhu, W. & Trolier-McKinstry, S. (2020). Comparative solution synthesis of Mn doped (Na, K) NbO_3 thin films. *Chemistry–A European Journal*, 26(42), 9356-9364.

[5] Yang, J., Gao, Z., Liu, Y., Xiong, Z., Zhang, F., Fu, Z. & Fang, L. (2021). Time dependence of domain structures in potassium sodium niobate-based piezoelectric ceramics. *RSC Advances*, 11(33), 20057-20062.

[6] Zhang, D., Zheng, F., Yang, X., Feng, L., Huang, X., Liu, H. & Cao, M. (2014). Preparation and ferroelectric properties of $K_{0.5}$ $Na_{0.5}$ NbO_3 thin films derived from non-alcohol niobium salt sol-gel process. *Integrated Ferroelectrics*, 154(1), 97-102.

[7] Wiegand, S., Flege, S., Baake, O. & Ensinger, W. (2012). Influence of different heat treatment programs on properties of sol–gel synthesized ($Na_{0.5}$ $K_{0.5}$) NbO_3 (KNN) thin films. *Bulletin of Materials Science*, 35, 745-750.

[8] Lai, F., Li, J. F., Zhu, Z. X. & Xu, Y. (2009). Influence of Li content on electrical properties of highly piezoelectric (Li, K, Na) NbO_3 thin films prepared by sol-gel processing. *Journal of Applied Physics*, 106(6), 064101.

[9] Sun, Y., Guo, F., Lu, Q. & Zhao, S. (2018). Improved ferroelectric photovoltaic effect in Mn-doped lead-free $K_{0.5}Na_{0.5}NbO_3$ films. *Ceramics International*, 44(12), 13994-13998.

[10] Deng, Y., Wang, J., Zhang, C., Ma, H., Bai, C., Liu, D. & Yang, B. (2020). Structural and electric properties of MnO_2-doped KNN-LT lead-free piezoelectric ceramics. *Crystals*, 10(8), 705.

[11] Akmal, M. H. M. & Warikh, A. R. M. (2021). Electrical behaviour of yttrium-doped potassium sodium niobate thin film for piezoelectric energy harvester applications. *Journal of the Australian*

Ceramic Society, 57(2), 589–596.

[12] Sharma, S., Gupta, R. & Tomar, M. (2022). Lattice-strain engineered $K_xNa_{1-x}NbO_3$ thin films near the morphotropic phase boundary for enhanced electrical properties. *Materials Chemistry and Physics*, 277, 125512.

[13] Aniz, I. M. & Maisnam, M. (2024). The effect of ZnO and MnO_2 as sintering aids in the preparation of potassium sodium niobate ceramics and electrical characterizations. *Ferroelectrics*, 618(1), 200–210.

[14] Amakali, T., Daniel, L. S., Uahengo, V., Dzade, N. Y. & De Leeuw, N. H. (2020). Structural and optical properties of ZnO thin films prepared by molecular precursor and sol–gel methods. *Crystals*, 10(2), 132.

[15] Helth Gaukås, N., Dale, S. M., Ræder, T. M., Toresen, A., Holmestad, R., Glaum, J. & Grande, T. (2019). Controlling phase purity and texture of $K_{0.5}Na_{0.5}NbO_3$ thin films by aqueous chemical solution deposition. *Materials*, 12(13), 2042.

[16] Wang, L., Ren, W., Goh, P. C., Yao, K., Shi, P., Wu, X. & Yao, X. (2013). Structures and electrical properties of Mn-and Co-doped lead-free ferroelectric $K_{0.5}Na_{0.5}NbO_3$ films prepared by a chemical solution deposition method. *Thin solid films*, 537, 65-69.

[17] Won, S. S., Lee, J., Venugopal, V., Kim, D. J., Lee, J., Kim, I. W., Kingon, A. I. & Kim, S. H. (2016). Lead-free Mn-doped ($K_{0.5}$, $Na_{0.5}$) NbO_3 piezoelectric thin films for MEMS-based vibrational energy harvester applications. *Applied Physics Letters*, 108(23), 232908.

[18] Ramajo, L. A., Taub, J. & Castro, M. S. (2014). Effect of ZnO addition on the structure, microstructure and dielectric and piezoelectric properties of $K_{0.5}Na_{0.5}NbO_3$ ceramics. *Materials Research*, 17, 728-733.

[19] Azman, M. A. H., Abd Rashid, M. W., Azlan, U. A. A., Shamsuri, S. R., Dom, A. H. M., Kassim, S. R., Harttar, M. A. M. & Hatta, M. (2024). Effect of Manganese dopant on the structure and electrical properties of Potassium Sodium Niobate thin film. *Malaysian Journal of Microscopy*, 20(1), 317-327.

[20] Li, J. W., Liu, Y. X., Thong, H. C., Du, Z., Li, Z., Zhu, Z. X., Nie, J. K., Geng, J. F., Gong, W. & Wang, K. (2020). Effect of ZnO doping on (K, Na) NbO_3-based lead-free piezoceramics: Enhanced ferroelectric and piezoelectric performance. *Journal of Alloys and Compounds*, 847, 155936.

[21] Hayati, R. & Barzegar, A. (2010). Microstructure and electrical properties of lead-free potassium sodium niobate piezoceramics with nano ZnO additive. *Materials Science and Engineering: B*, 172(2), 121-126.

[22] Ammaih, Y., Lfakir, A., Hartiti, B., Ridah, A., Thevenin, P. & Siadat, M. (2014). Structural, optical and electrical properties of ZnO: Al thin films for optoelectronic applications. *Optical and Quantum Electronics*, 46, 229-234.